A molecular information ratchet using a cone-shaped macrocycle

Enxu Liu, Sawsen Cherraben, Laora Boulo, Claire Troufflard, Bernold Hasenknopf, Guillaume Vives, Matthieu Sollogoub

A molecular information ratchet using a cone-shaped macrocycle

Enxu Liu,[†] Sawsen Cherraben,[†] Laora Boulo, Claire Troufflard, Bernold Hasenknopf, Guillaume Vives,* Matthieu Sollogoub*

Sorbonne Université, CNRS, Institut Parisien de Chimie Moléculaire (IPCM), UMR 8232, 4 place Jussieu, 75005 Paris, France

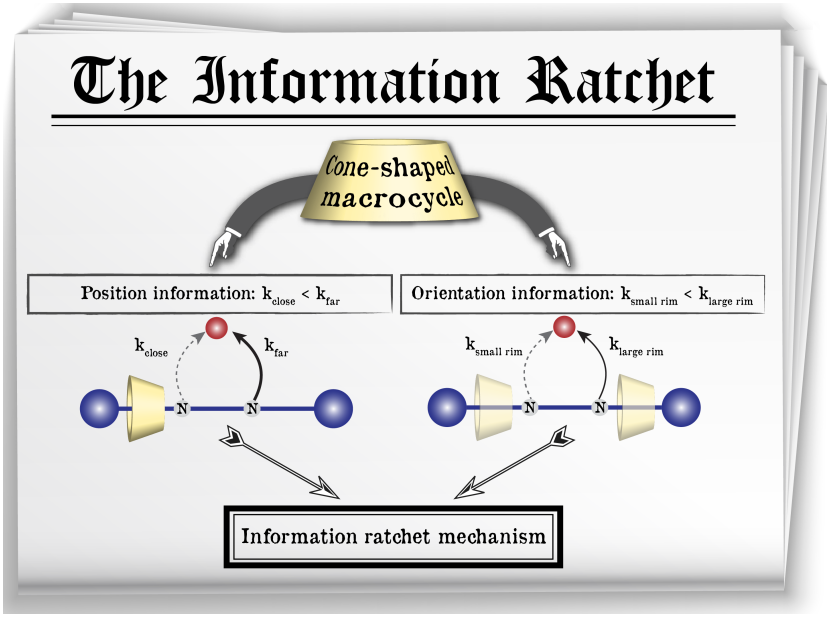

Abstract: Molecular information ratchets are key to the construction of autonomous chemically fuelled small-molecule motors. We have developed a novel type of information ratchet, sensitive to two types of information: both the position and the orientation of a moving macrocycle on an axle. The originality of this system comes from the use of a cone-shaped chiral macrocycle, a cyclodextrin, that presents two distinct faces towards the reactive site, and is responsible for the kinetic biases observed. The reaction of functional groups on the axle next to the larger rim was found to be faster than that next to the smaller rim. An additional advantage of the conical shape of cyclodextrins is the possibility of selective face functionalization allowing the addition of a component that will be active in the kinetic bias, which will improve the ratchet efficiency, thu offering new possibilities in the design of molecular motors.

Keywords: Cyclodextrin, rotaxane, molecular machine, ratchet, supramolecular chemistry

Introduction

[†] These authors contributed equally.

Essential to life, kinesin and ATP synthase are both proteins that undergo unidirectional movement. Fascinated by Nature's ability to build such molecular machines, and inspired by Feynman's challenge to build "tiny machines with movable parts", some time ago, chemists set out to design such molecular objects.[1,2] A whole field was subsequently developed, and numerous machines have been built, for example, pumps,[3-5] rotors,[6] muscles,[7] walkers,[8] transporters,[9,10] and switches.[11] Indeed, this field was recently recognized by the award of a Nobel prize to some of its pioneers. Among all the molecular machines made to date the most fascinating and challenging are the motors,[12] which rotate with net directionality by consuming energy and performing work. To date only a few motors with unidirectional movement have been created.[13-18] These have been based on two main design features, which involve either controlled rotation of the rotor moiety around a single or double bond, or rotation of a ring interlocked into another ring in a catenane architecture. These motors function by successive reactions that sequentially modify the energy profile, and therefore induce unidirectional movement through what has been termed 'an energy ratchet'.[19] One remarkable exception to these two established designs is the autonomous chemically-fuelled small molecule motor developed by Leigh that continuously rotates with net directionality.[20] In order to construct such a system Leigh first had to develop a chemically-driven information ratchet.[21,22] The difference between energy and information ratchets is that in the former the energy profile of the process is modified by an external stimulus independently of the position of the moving entity, while in the latter the energy profile of the process is dependent on the position of the moving molecular entity.[23,24] Leigh developed his information ratchet using a [2]rotaxane,[25] i.e. a macrocycle threaded on an axle. He first designed a prochiral axle with two equivalent stations that were separated by a prochiral hydroxyl group which, in the presence of the macrocycle and upon reaction with an anhydride and a chiral base, acted as an information ratchet. He showed that the rate of the reaction was sensitive to the position of the macrocycle on the axle, because the direction of approach of the anhydride towards the hydroxyl group on the axle was controlled by the chirality of the base. The position of the macrocycle constitutes the information given to the ratchet to operate. Starting from an even distribution of the macrocycle at both stations, the information ratchet produced different distributions at the stations, driving the system away from the even distribution at the equilibrium of the starting rotaxane through kinetic resolution of the two mechano-enantiomers (Scheme 1a). The same ratcheting mechanism was extended to a rotaxane with three stations and two ratchets, which allowed double ratcheting and transport over longer distances.[26] Very recently, an autonomous rotaxane-based information ratchet was developed to progressively pump the macrocycle distribution away from equilibrium using a carbodiimide fuel.[27] Building on these results Leigh developed an autonomous chemically fuelled motor.[20] For a given reaction the ratchet is only sensitive to the position of the achiral 2D macrocycle on the axle. As all of these systems are based on 2D achiral macrocycles, we therefore wondered if we could develop an information ratchet that would be sensitive both to the position and the face of the macrocycle, thus introducing the asymmetry into the moving entity. To this end we envisaged the use of a chiral 3D macrocycle that could be threaded onto an achiral symmetrical axle, and so would present two different faces to the reactive

centre. Cone-shaped macrocycles appeared attractive for such application as they could induce directional control into a switch by exploiting the difference in ground state energy between two co-conformers.[28,29] Among possible 3D macrocycles we selected cyclodextrins (CDs) as they are cone-shaped, chiral, readily available, and cheap. While CDs have been widely used to form rotaxanes,[30-34] use of their asymmetry to induce directional motion in molecular machines has not been thoroughly investigated.[35]

Herein, we describe the production of CD-based [2]rotaxanes which exhibit an information ratchet mechanism with dual inputs from the moving macrocycle, namely (i) the position of the CD on the axle and (ii) the orientation of the cone-shaped CD relative to the ratchet. The rotaxanes are composed of two stoppers and three alkyl segments separated by two secondary amines which will react with an achiral reagent to operate as information ratchets (Scheme 1b). This study therefore represents a different approach to Leigh's seminal chemical information ratchets, as in that case chiral information was brought by an external component, and therefore the information provided to the ratchet for any given reaction, was only the position of the macrocycle.

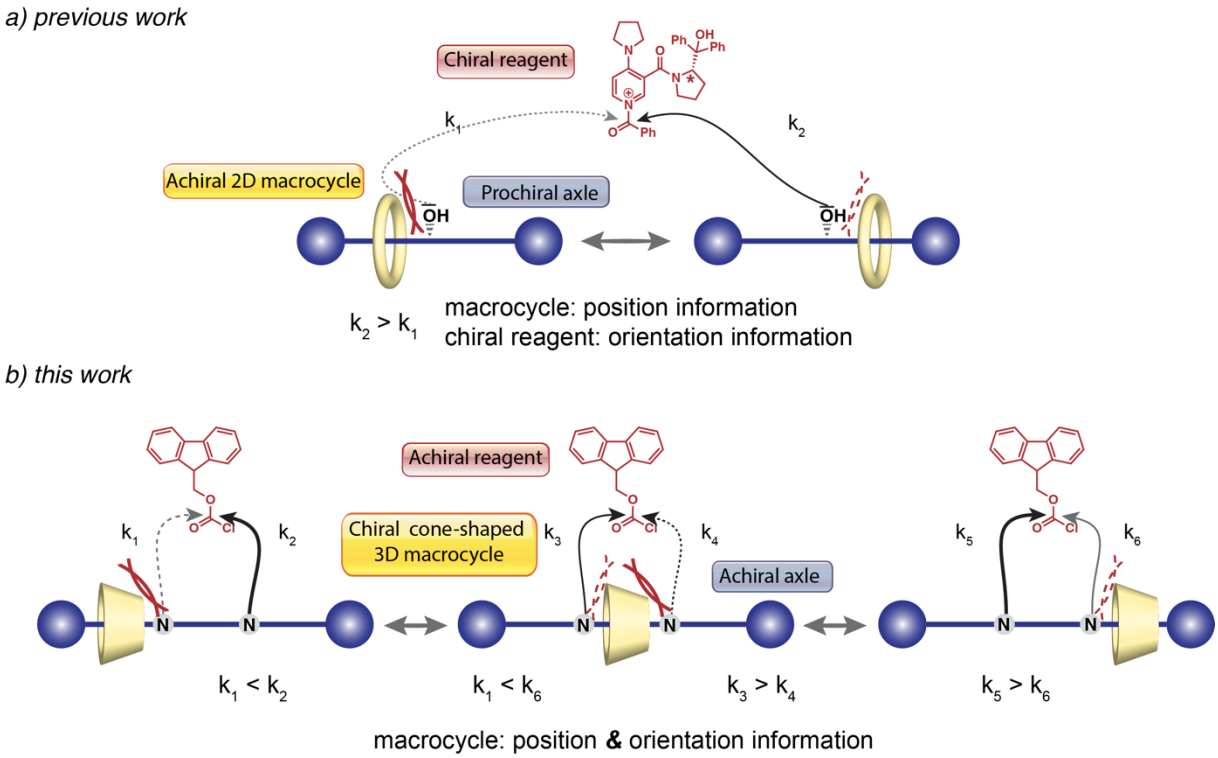

Scheme 1: a) Leigh's information ratchet based on the position of a macrocycle on a prochiral axle reacting with a chiral reagent;[25] b) Information ratchet developed here, based on the position and orientation of a cone-shaped macrocycle threaded onto on an achiral axle reacting with an achiral reagent.

Results

Synthesis. The target CD [2]rotaxanes **10** and **11** with three compartments were synthesized by a strategy involving rotaxanation and post-functionalization (Scheme 2). Permethylated α-CD was selected as the macrocycle instead of native α-CD in order to avoid side reactions of the hydroxyl groups, and to allow the use of organic solvents both for the post-functionalization of the rotaxane and the operation of the ratchet. However, only a few examples of permethylated CD-based rotaxanes have been reported, probably due to their relatively low affinity with hosts in water. Actually, the highest yield for the production of a permethylated α-CD [2]rotaxane was reported by Takata using bisamino-dodecane axle and a urea end-capping reaction.[36] We therefore decided to apply this synthesis to first form a rotaxane with a central 12 carbon segment (**4**), and then to post-functionalize by attaching segments to both ends. Our objective was to produce a rotaxane comprising an axle with three segments of similar affinities to minimize any thermodynamic bias to the motion of the CD-macrocyle. For the two additional side segments, we decided to investigate two cases: either using one comprising an 8-carbon chain, a triazole, and a di-tertbutyl phenyl stopper (**10**), or a 12-carbon chain, the triazole and the stopper (**11**). Therefore first permethylated α-CD **1** and diaminododecane **2** were mixed in aqueous 0.1 M NaOH solution to form the pseudo-rotaxane. Then the primary amines were reacted with dimethylbenzyl chloride **3** to form the [2]rotaxane **4** in 38% yield. This procedure was inspired both by Takata for the diamine axle,[36] and Stoddart[37] for the stoppering reaction[38] which forms amides instead of urea, and so allows further post-functionalization. NOE cross-correlation between the CH_2 chain protons of the axle and inwardly orientated H^5 of the CD confirmed the threading and the formation of **4** (Figure S1). Amide **4** was then treated with $LiAlH_4$ to reduce the amides into amines and form **5** in 80% yield. The secondary amines were then used to introduce the two other alkyl segments through reductive amination. Reaction between **5** and aldehydes **6** or **7** (see SI, scheme S1) in the presence of $NaBH(OAc)_3$ in DCM gave **8** and **9** in 75% and 65% yields, respectively. Finally, the dimethylbenzyl groups of **8** and **9** were removed *via* hydrogenolysis to form **10** and **11** in 45% and 35% yields, respectively. The achiral, symmetrical axle makes each of **10** and **11** a single mechanoisomer of CD-based [2]rotaxanes (Scheme 2).

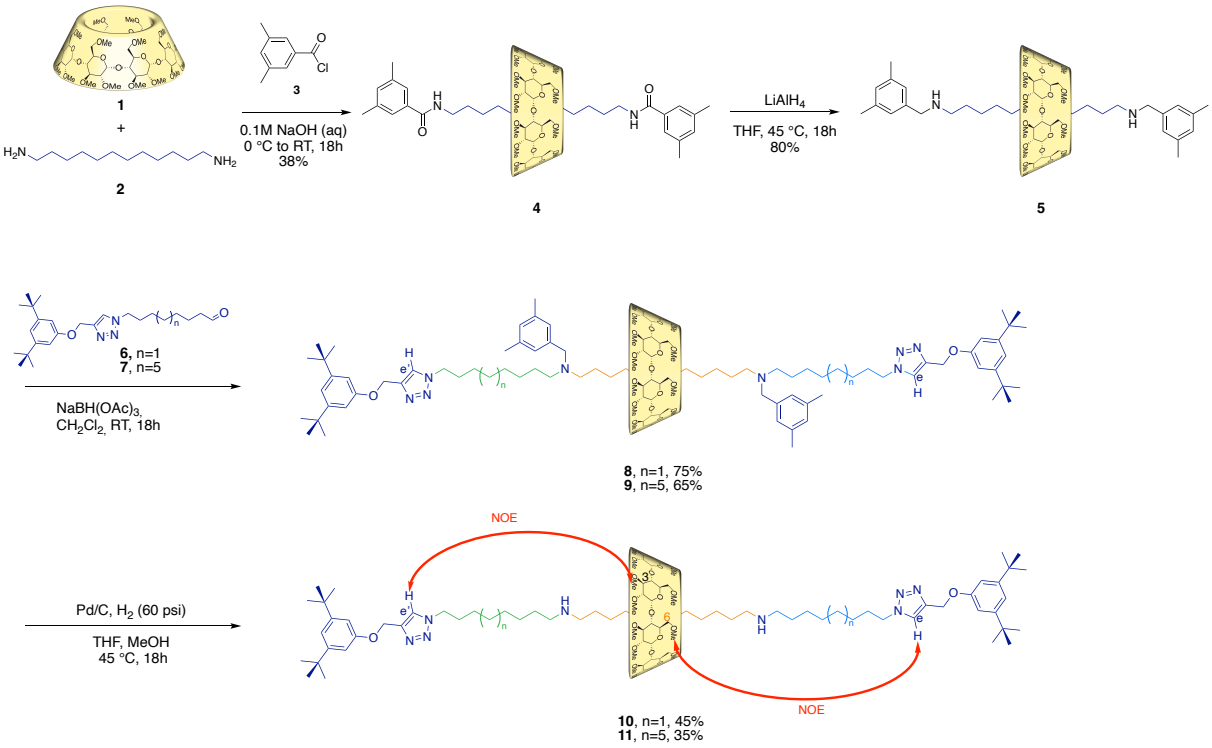

Scheme 2. Synthetic route to rotaxanes **10** and **11**.

The rotaxanes were fully characterized by NMR and high-resolution mass spectrometry. NOE analysis was performed on both rotaxanes **10** and **11** and confirmed the shuttling of the CD along the entire axle as both imidazole protons H^e and $H^{e'}$, present at either end of the axle, displayed cross-correlations with CD protons. In accordance with expected proximities based on structure, the methoxy groups situated on the primary rim and the H^5s correlated with H^e, while the methoxy groups at position-3 of the CD correlated with $H^{e'}$ (Figure S2, S3).

Fmoc-protection. We next protected the amines of rotaxanes **10** and **11** with Fmoc groups to introduce steric barriers between the three segments. Therefore, as we had so far observed the shuttling of the CD along the entire length of the axle, the formation of three mechanoisomers, **A**, **B**, **C** for both **12** and **13** was expected. Compounds **12A-12C** and **13A-13C** possess two types of chirality: the stereogenic centres of the sugars constituting the CD, and the mechanical planar chirality of the rotaxane due to the orientation of the CD. Therefore, mechanoisomers **12A-12C** and **13A-13C** are mechanically planar chiral diastereomers[39] (Scheme 3). Diamine **10** was initially reacted with Fmoc-Cl and N,N-diisopropylethylamine (DiPEA) as base in DCM at RT. Analysis of the product by ^{1}H NMR revealed splitting of the signal of protons belonging to both the CD and the axle. Of particular interest, in the case of **12A-C**, the triazole proton $H^{e'}$ for **12C** appeared as a distinct peak, and the methyl groups at O^6 of the CD were split in two. However, no trace of a third set of signals was observed by NMR. We therefore concluded that somewhat surprisingly the reaction had produced only two mechanoisomers (Figure 1a). Each set of protons could be attributed to mechanoisomers **12B** and **12C** by 2D NOESY, COSY and TOCSY experiments (Figure 1b and for details see SI, Figure S4-S12).

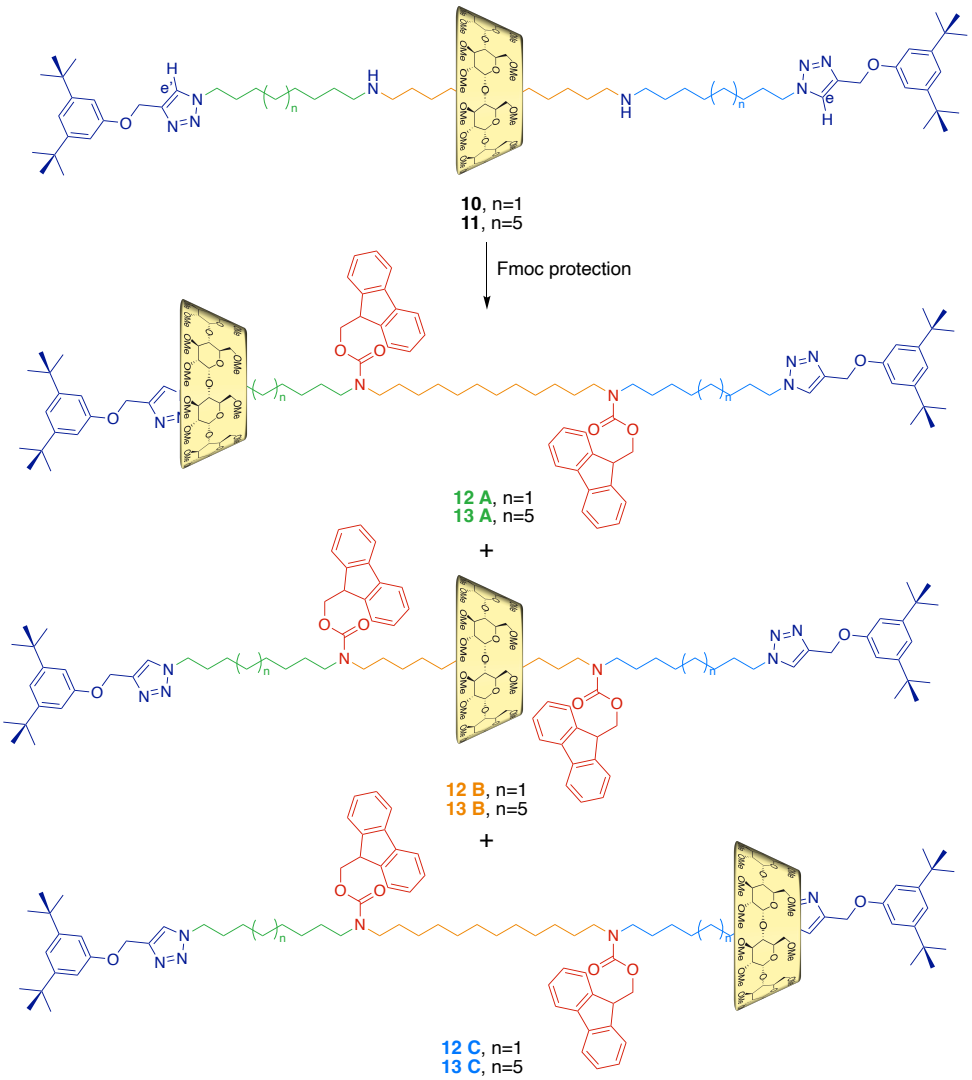

Scheme 3. Fmoc protection of [2]Rotaxanes **10** and **11**.

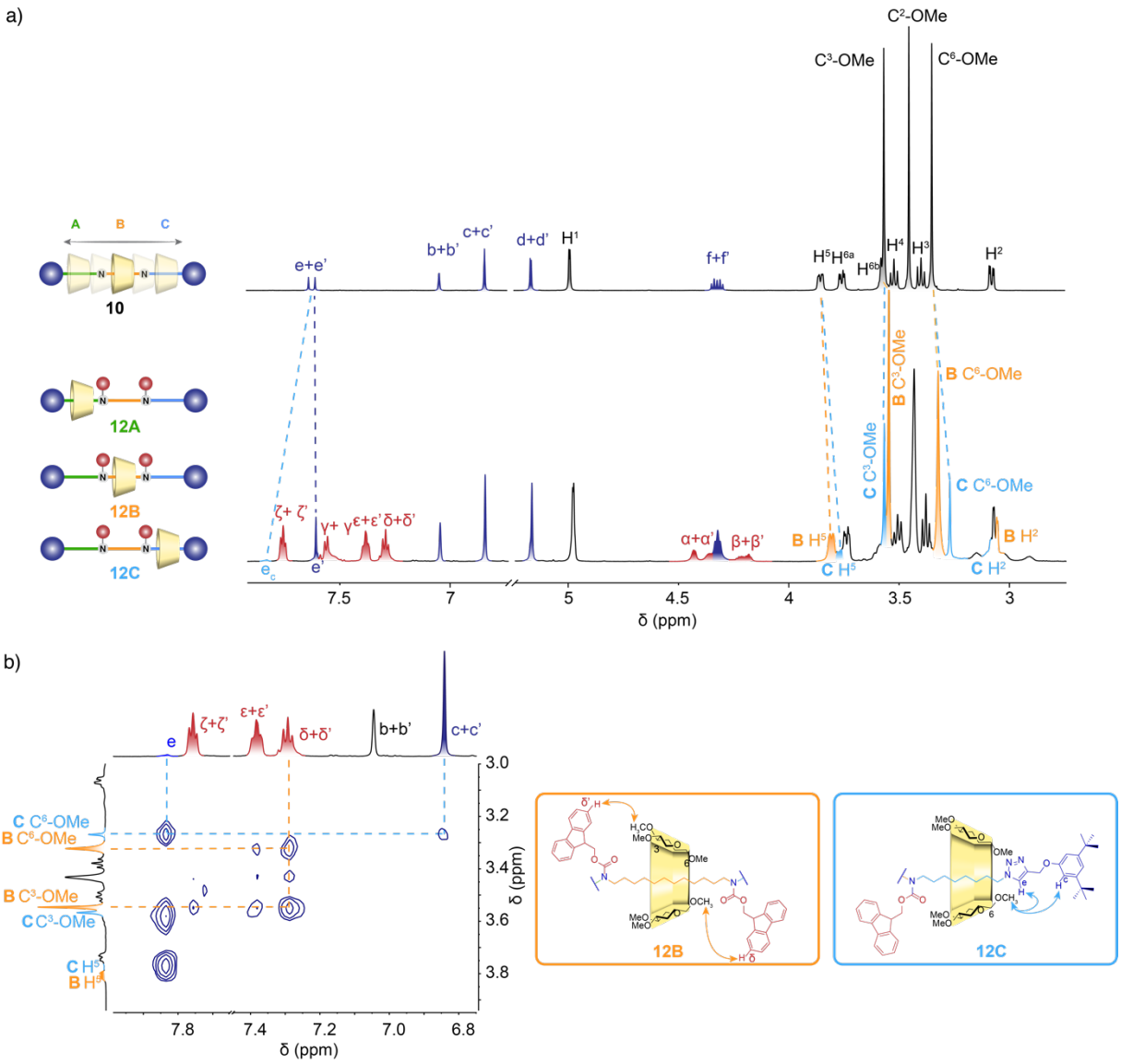

Figure 1. a) ^{1}H NMR (600 MHz, CD_2Cl_2) spectra of **10** and mechanoisomers **12** (**A**/**B**/**C**=trace/77/23). b) Partial NOESY NMR spectrum (600MHz, CD_2Cl_2) of **12** (**A**/**B**/**C**=trace/77/23) allowing the attribution of mechanoisomers **B** and **C**.

Next, any effect on the ratio of **12B** to **12C** produced was investigated by variation of reaction parameters, including the temperature, solvent, the Fmoc derivative used, and the base (Table 1). Notably, the nature of the base used had no influence on the product distribution (Table 1, entries 1-3 and 4-7). The Fmoc derivatives, differentiated by their leaving groups, had only a marginal influence on product distribution (entry 2 vs 11-13). However, a significant variation of reaction mechanostereoselectivity was observed by changing either the solvent (Figure S13, Table 1, entry 2 vs 4 vs 8) or the temperature (table 1, entry 2 vs 9-10). As stated above, in DCM **12A** was only formed in trace amounts in DCM and a 77:23 ratio of **12B:12C** was observed. In THF, the proportion of **12C** formed was the highest (39%), while it was the lowest (16%) in acetonitrile (Table 1). The effect of temperature was investigated by performing the reaction in DCM with Fmoc-Cl and DiPEA at three different

temperatures. Upon lowering the temperature in DCM, the proportion of **12C** was gradually reduced from 23% at RT to 9% at -60 °C.

Table 1. Reaction conditions for Fmoc protection on **10** and the corresponding ratio between mechanoisomers **12A**, **12B** and **12C**.

Entry	*Solvent*	*Temperature*	*Base*	*Fmoc derivatives*	*12A%*	*12B%*	*12C%*
1	DCM	RT	DiPEA+DMAP (10 equiv.)	FmocCl	Traces	77	23
2[a]	DCM	RT	DiPEA	FmocCl	Traces	77	23
3	DCM	RT	NEt_3	FmocCl	Traces	77	23
4[a]	THF	RT	DiPEA	FmocCl	Traces	61	39
5	THF	RT	NEt_3	FmocCl	Traces	61	39
6	THF	RT	Na_2CO_3 (s)	FmocCl	Traces	61	39
7	THF	RT	DiPEA+DBU (cat.)	FmocCl	Traces	61	39
8[a]	MeCN	RT	DiPEA	FmocCl	Traces	84	16
9	DCM	-20°C	DiPEA	FmocCl	Traces	85	15
10	DCM	-60°C	DiPEA	FmocCl	Traces	91	9
11	DCM	RT	DiPEA	Fmoc-O-succinimide	Traces	78	22
12	DCM	RT	DiPEA	Fmoc-O-benzotriazole	Traces	80	20
13	DCM	RT	DiPEA	Fmoc-O-C_6F_5	Traces	74	26
14	THF	RT	DiPEA	Fmoc-O-C_6F_5	Traces	62	38
15	MeCN	RT	DiPEA	Fmoc-O-C_6F_5	Traces	84	16

[a] *These experiments were performed at least three times with results within ±1%.*

Since isomer **12A** was barely detectable, regardless of the conditions used for N-protection of rotaxane **10**, reaction mechanoselectivity was further investigated using rotaxane **11** which comprises longer hydrocarbon side chains. Under the same reaction conditions, reaction of **11** produced NMR spectra showing three sets of signals, most clearly visible for the C^3-OMe protons, indicating in this case the formation of three mechanoisomers (Figure 2a and Fig. S14-22). Each set of signals was attributed to its corresponding isomer by the analysis of NOE correlations between the CD and protons of either the Fmoc or stopper groups (Figure 2b). The ratio of **13A**, **13B** and **13C** formed was determined by the relative sizes of the integrals corresponding to three ortho-protons on the di-tertbutylphenyl stopper. We also studied the effects of solvent, temperature, and Fmoc-reagent on product distribution (Table 2). The effects observed were similar to the case of **10**, with additional formation of quantities of isomer **A**.

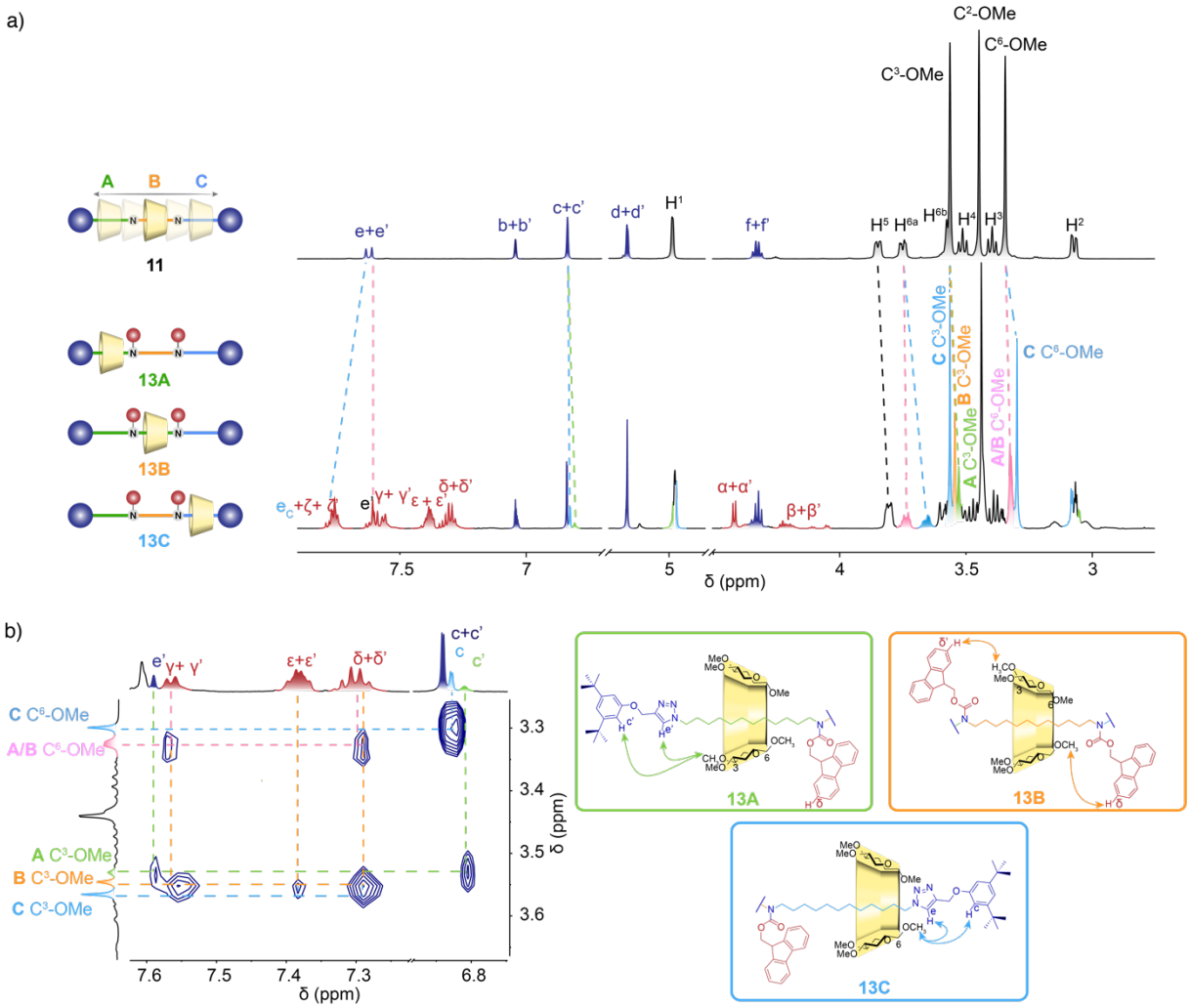

Figure 2. a) ^{1}H NMR (600 MHz, CD_2Cl_2) spectra of **11** and mechanoisomers **13** (**A**/**B**/**C**=16/27/57). b) Partial NOESY NMR spectrum (600MHz, CD_2Cl_2) of **13A-C**

Table 2. Reaction conditions for Fmoc protection of **11** and the corresponding ratio between mechanoisomers **13A**, **13B** and **13C**.

Entry	*Solvent*	*Temperature*	*Base*	*Fmoc derivatives*	*Mechanoisomer*		
					13A%	**13B**%	**13C**%
1[a]	DCM	RT	DiPEA	FmocCl	26	30	44
2[a]	MeCN	RT	DiPEA	FmocCl	16	44	40
3[a]	THF	RT	DiPEA	FmocCl	16	27	57
4	DCM	-20°C	DiPEA	FmocCl	19	43	38
5	DCM	RT	DiPEA	$FmocOC_6F_5$	23	30	47
6	MeCN	RT	DiPEA	$FmocOC_6F_5$	18	34	48
7	THF	RT	DiPEA	$FmocOC_6F_5$	20	20	60

[a] *These experiments were performed at least three times with results within ±1%.*

Initial distribution. In order to try and correlate the uneven distribution of isomers formed to a kinetic bias or not, we evaluated the occupancy of segment **C** in **10** (and **11**). The fast shuttling of the CD in **10** (and **11**) was demonstrated by use of the triazole protons serving as probes. The two triazole protons H^e and $H^{e'}$ appear as one singlet in the ^1H NMR spectrum of **8** (and **9**), because the shuttling of the CD is blocked by the two dimethylbenzyl stoppers on the central segment, preventing the triazole protons from sensing the asymmetry of the CD (Figure 3a). However, once the two dimethylbenzyl stoppers have been removed to form **10** (and **11**), the triazole protons H^e and $H^{e'}$ split into two singlets, one upfield and the other downfield of the corresponding signal in the spectrum of **8** (and **9**), indicating rapid-shuttling of the CD at RT (Figure 3b). Moreover, NOE correlations of $H^{e'}$ with the C^3-OCH_3 and H^e with the C^6-OCH_3 protons of the CD were observed, indicating that the CD can shuttle from one triazole to the other along the axle (Scheme 2, Figure S2-3). Therefore in **10** (and **11**) the CD is distributed over the three segments **A**, **B** and **C**. However, as the three co-conformers **10A**, **10B** and **10C** (**11A**, **11B** and **11C**) are diastereomers the distribution between the three segments of the axle might be uneven. A complication in assessing this distribution is the absence of any specific interaction between the CD and the axle in organic solvents, and therefore in **10** (and **11**) there is no preferred location for the CD to reside in. We therefore used the triazole protons as probes as they mark the extremities of the axle, and should be sensitive to the proximity of the CD. Compound **8** (and **9**) was therefore used as guide for the triazole proton chemical shift with 0% occupancy of segment **C** by the CD, whereas the chemical shift for a triazole surrounded by CD with 100% occupancy was inferred from rotaxane **12C** (and **13C**) (Figure 3c). The occupancy of segment **C** was estimated using these extremes using a fast exchange model in all of the solvents studied (Figure 3, Table 3, Figure S23). However, the occupancy of the other segments could not be determined using this method. First of all, as **12A** had not been observed the chemical shift for the triazole with 100% occupancy of segment **A** was unavailable. Additionally, for **13A** the triazole proton $H^{e'}$ overlapped with those of the Fmoc groups and the triazole protons of the other mechanoisomers, precluding accurate estimation. Finally, for segment **B**, no distinctive proton signal could be used to estimate segment occupancy.

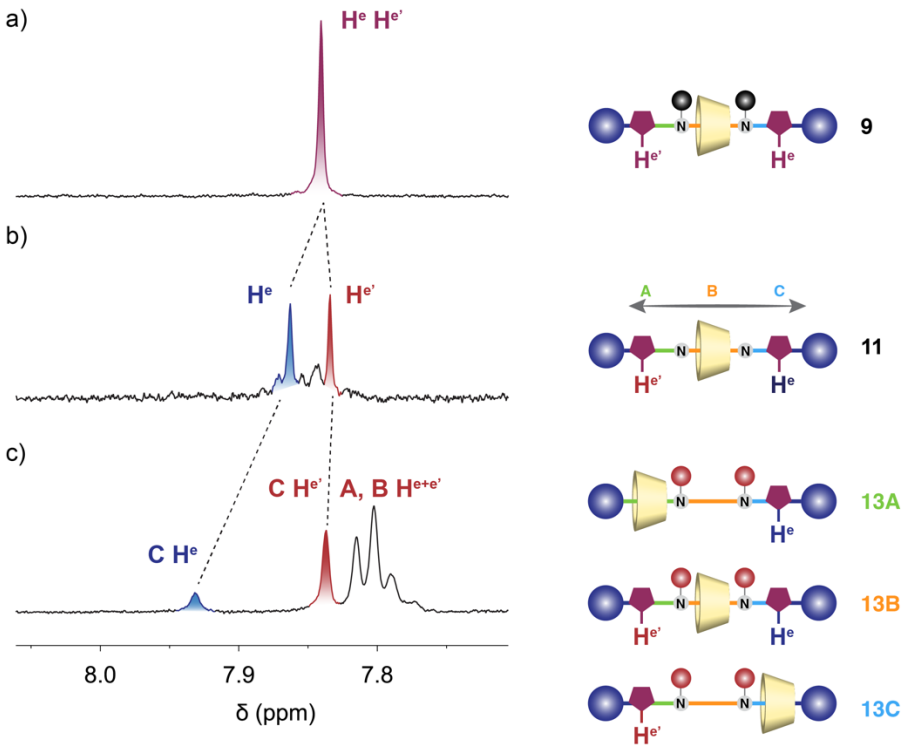

Figure 3. ^{1}H NMR spectra (600MHz, THF-d_8) showing the influence of position of the CD on the chemical shift of triazole protons H_e and $H_{e'}$ in rotaxanes a) **9**, b) **11** and c) **13**.

Table 3. Comparison of the estimated occupancy of segment **C** in **10** and **11**, and the ratio of **12C** and **13C** mechanoisomers formed after Fmoc-Cl protection reaction at RT.

Solvent	Occupancy of segment C in **10**	ratio of **12C**	Occupancy of segment C in **11**	ratio of **13C**
MeCN-d_3	16%	16%	21%	40%
CD_2Cl_2	13%	23%	18%	44%
THF-d_8	24%	39%	24%	57%

From Table 3 it is clear that the proportion of occupancy of segment **C** when the CD can freely shuttle on the axle in **10** and **11** is significantly different from that of **12C** and **13C** after Fmoc-protection. Such changes in occupancy and the absence of isomer **12A** strongly points toward a kinetic bias in the Fmoc-protection reaction. However, the protection of the two amines is a two-step process, thus complicating direct interpretation of the product distribution. To better understand this process, we also sought to study the Fmoc-protection on model mono-*N*-benzylated compounds **16-19**, which were obtained when rotaxanes **8** and **9** were submitted to hydrogenolysis under the same conditions used to form **10** and **11** but for only 2h rather than for 12h. In each case, we isolated a small quantity of an approximately equimolar ratio of both monobenzylated regioisomers, namely compounds **16**, **17** and **18**, **19**, respectively. NOE analysis performed on rotaxanes **16-19** confirmed the *N*-benzyl group acted as a stopper and also provided evidence of shuttling of the CD between the remaining accessible

segments (Figure S24 and S25). These mixtures were then reacted with FmocCl in the presence of DIPEA and at RT to afford mixtures of two pairs of mechanoisomers **20A,B** and **21B,C** from **16, 17** and **22A,B** and **23B,C** from **18,19** (Scheme 4).

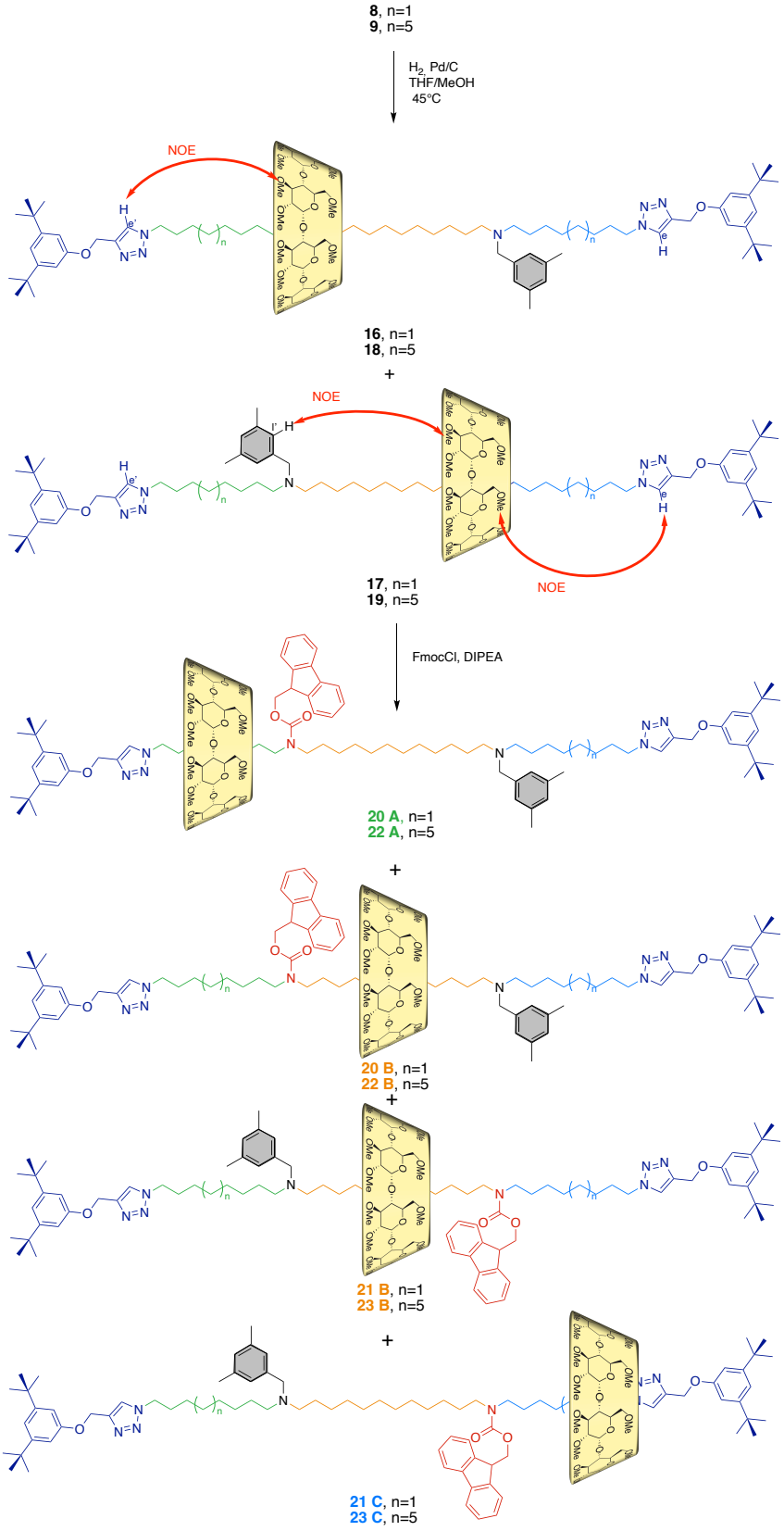

Scheme 4. Synthesis and Fmoc protection of monobenzylated rotaxanes **16-19**.

For the rotaxanes containing the C_8 axle segment, the reaction of the 1:1 mixture of the monobenzylamines **16:17** with FmocCl gave a mixture of 3 products, identified as **20B**, **21B** and **21C**, and only traces of **20A**. In fact, compounds **20B** and **21B** could not be distinguished by NMR, but since **20A** was not formed, it was assumed that the proportion of **20B** produced corresponded to that of **16** used in the reaction. In this case, reaction of **17** afforded less **21C** than **21B**, a result that is in agreement with the production of **12C** from **10** in only minor amounts. When these Fmoc protection conditions were applied to the 1:1 mixture of **18** and **19** a mixture of 4 products was obtained. This time, **22B** and **23C** were obtained in higher proportions than **22A** and **23B** respectively (Scheme 4, Table 4).

Table 4. Proportions of mechanoisomers formed after Fmoc protection of monobenzylated compound with DiPEA and FmocCl in different solvents at RT.

Solvent	**Rotaxane**	**20A**	**20B**	**Rotaxane**	**21B**	**21C**
DCM	**16**	Traces	100%	**17**	70%	30%
THF	**16**	Traces	100%	**17**	52%	48%
Solvent	**Rotaxane**	**22A**	**22B**	**Rotaxane**	**23B**	**23C**
DCM	**18**	42%	58%	**19**	48%	52%
THF	**18**	48%	52%	**19**	36%	64%

To deduce the ratios of the rate constants from these results, we needed to study the initial distributions of the mechanoisomers of **16-19**. As previously described, the chemical shift of the triazole protons H^e was used as a probe to estimate the occupancy of segment **C** in monobenzylated rotaxanes **17** and **19** (Table 5). The significant difference between the occupancy of segment **C** in starting materials **17** and **19** and products **21C** and **23C** indicates some kinetic bias during the Fmoc protection. We analysed this transformation as a dynamic kinetic resolution of two mecano-diastereoisomers assuming a simple Curtin-Hammett principle that the shuttling equilibrium between the co-conformers of **17**,**19** was much faster than the Fmoc reaction, and that Fmoc protection was irreversible.

Table 5. Comparison of the estimated occupancies of segment C in **17** and **19** and the ratios of **21C** and **23C** mechanoisomers formed after Fmoc protection at RT.

Solvent	Occupancy of segment C in **17**	yield of **21C**	Occupancy of segment C in **19**	yield of **23C**
CD_2Cl_2	23%	30%	26%	52%
THF-d_8	36%	48%	44%	64%

Discussion

In order to provide further insight into the dynamics of this molecular system we estimated the rate of shuttling of the CD on the axle by VT-NMR. No coalescence of the ^{1}H NMR spectra of **10** was observed in CD_2Cl_2 even at temperatures as low as 190 K, indicating fast shuttling with an energy barrier <10

kcalmol^{-1}. By comparison with similar systems in the literature,[40,41] the rate constant of the shuttling was therefore estimated to be >10^6 s^1. Furthermore, we observed a $t_{1/2}$ for the Fmoc protection reaction at 213 K that was in the range of 30 min. Therefore, it is assumed that shuttling of the CD along the axle is much faster than the N-protection.[20] Additionally, no N-Fmoc deprotection of **12A-C** and **13A-C** was observed in either DCM or THF, even after the reaction was left for multiple days. Therefore, it can be concluded that the Fmoc-protection reactions converting **10** into **12**, and **11** into **13**, are not reversible and the product distribution is therefore under kinetic control. It is worth noting that according to the Curtin-Hammett principle[42-44] although the reaction is under kinetic control, the equilibrium constant between co-conformers of **10** and **11** will have an influence on the distribution of products **12A-C** and **13A-C**

To decipher the respective influences of the kinetics and equilibrium constants on the outcome of the protection reactions, we first analysed the reaction of the simpler model compounds **16-19**. For the conversion of **17** into **19** (Scheme 5a), we deduced an equilibrium constant of K = 0.30 for the initial distribution of **17B** and **17C** in DCM, and similarly for the equilibrium between **19B** and **19C** (K = 0.35). From the product distribution and the Curtin-Hammett equation, we deduced the ratio of kinetic constants. Hence $k'_C/k'_B = 1.4$ in the case of the C_8 derivative **17** and this ratio increased to 3 for the C_{12} compound **19**. This difference in rate allows the enrichment of products **21C** and **23C** as compared to the initial distribution of co-conformers. The same process was repeated in THF and we consistently observed that $k'_C > k'_B$ (Table 6). In all cases, we observed that the reaction to form the product where the CD ended up on segment **C** was faster, and this increased rate was higher for the C_{12} derivatives. We can relate this increase to the difference of lengths of the segment **C**. Indeed, the steric hindrance generated by the secondary rim of the CD on the reacting amine group is lower when the CD is located on the longer **C** segment of **19** as compared to **17**. (Table 6)

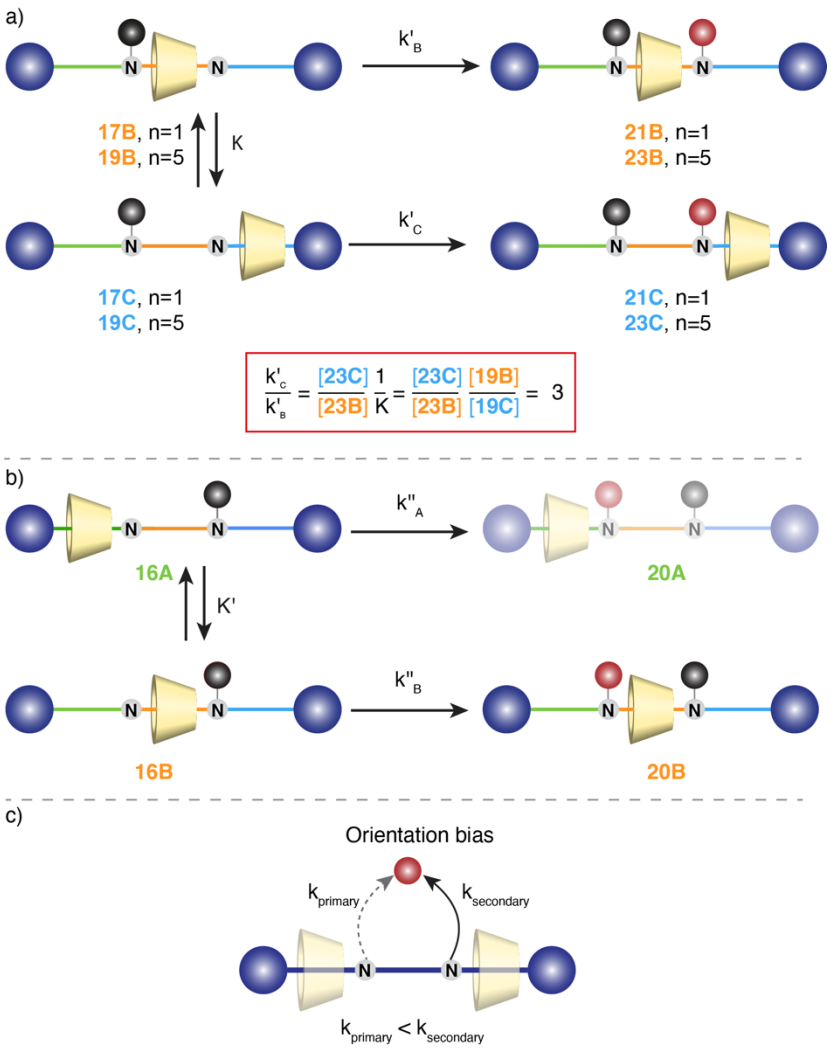

Scheme 5. a) Dynamics of the Fmoc protection reaction of monobenzylated rotaxanes **17** and **19**, and calculation of the relative rates in DCM. b) Proposed orientation bias where the kinetics of Fmoc protection are faster when the secondary rim is facing the anchoring site, as opposed to when the primary rim faces the anchoring site. c) Dynamics of the Fmoc protection reaction of monobenzylated rotaxanes **16**.

Table 6. Evaluation of the thermodynamic and kinetic parameters for the Fmoc-protection reaction of compounds **17** and **19** in DCM and THF.

Solvent	K **17C/17B**	k'_C/k'_B **21C/21B**	K **19C/19B**	k'_C/k'_B **23C/23B**
CD_2Cl_2	0.30	1.4	0.35	3.0
THF-d_8	0.56	1.7	0.78	2.3

A similar kinetic bias was observed in the reaction of **16** although it was not possible to quantify this as the initial distributions of **16A** and **16B** were not available. Nonetheless, while **16A** is present in equilibrium with **16B**, as demonstrated by NOE (Scheme 4, Figure S24), only product **20B** was detected after the reaction, indicating that $k'_{B1} >> k'_{A2}$ (Scheme 5b).

Nonetheless, these results explicitly show that the Fmoc protection reaction was faster when the larger

rim of the CD was facing towards the amine group, rather than when the smaller rim did. The existence of a kinetic bias based on the orientation of the CD has therefore been demonstrated in this instance. In fact, the present system corresponds to the definition of an information ratchet wherein the energy landscape of the reaction depends on the relative position of the moving entity. (Scheme 5c)

With this kinetic data in hand, analysis of the complete reaction pathway for the double Fmoc protection of compounds **10** and **11** (Scheme 6a) was undertaken, in an attempt to rationalize the observed product ratios (Tables 1 and 2). Reaction of **10** can be broken down in two steps; firstly the initial formation of four mono-Fmoc-protected intermediates **14a**, **14ba**, **14bc**, **14c**, which are then converted into the final di-Fmoc-protected mixtures of mechanoisomers **12A**, **12B**, **12C** (Scheme 6a). A similar analysis can be applied to reaction of **11**. There are two indicators that kinetic bias linked to the orientation of the CD on the axle is also at play in this system. First, the absence of any **12A** formed during the Fmoc-protection of **10**, although segment **A** is accessed by the CD, as shown by NOESY experiments (Figure S2, S3). This indicates that $k_a<k_c$ because the reaction of **16A**, the *N*-benzylated analogue of **14ba**, produces only **20B**, and therefore that $k_{A2}<<k_{B1}$. Hence, the *N*-protection reaction is slow when the CD is placed on the end segment with its small rim facing the amine. On the other hand, when the CD is facing the amine with its large rim the *N*-protection occurs faster, because isomer **12C** was produced in the final mixture in a higher proportion than the occupancy of segment **C** in **10**, therefore demonstrating $k_{C1}> k_{B2}$. This difference was even more pronounced for rotaxane **11**, where the final proportion of **13C** formed was more than twice that of the occupancy of segment **C** in **11**. Such a drastic change between segment occupancy and observed final product ratios strongly implies a kinetic bias in the Fmoc-protection reaction in the full system as well. However, the observed proportions of products cannot be fully account for using the orientation bias alone. A second bias, depending on the position of the CD on the axle needs to be implemented. For example, when the CD is on segment **A** the protection of the proximal amine is slower than that of the distal one, i.e. $k_{ba} > k_a$ and by the same reasoning $k_{bc} > k_c$. This equates to the straightforward hypothesis that the reaction of the amine is faster when the CD is far away from it (Schemes 6b, 6d). This position bias is actually the one already used by Leigh for his information ratchet.[26] Finally, the protection of the remaining amine in **14a** and **14c** should be faster than the other reactions ($k_{A1}\approx k_{C2}$ > all other k) as the CD is enforced to be distant from the reactive site, but this last step does not change the final ratio of products. Based on these three hypotheses, a set of kinetic constants that accounts for the observed product ratios for the double N-Fmoc protection of **10** and **11** in DCM and THF has been proposed (Figures S28, S29, S32, S33). From these models, it appears that orientation and position are linked as $k_{ba}<k_{bc}$ (Scheme 6a), it is therefore difficult to decompose the contribution of each bias. However, from the kinetics models, we find that k_a(**10**)/k_{ba}(**10**) < k_a(**11**)/k_{ba}(**11**), which shows that the position bias is stronger in the case of **10**. This observation is logical considering that **10** bears shorter side arms than those of **11**, and therefore when the CD is on position **A** in **10** the steric hindrance on the proximal amine is stronger than when the CD is on the same position in **11** thus the observed difference of ratio.

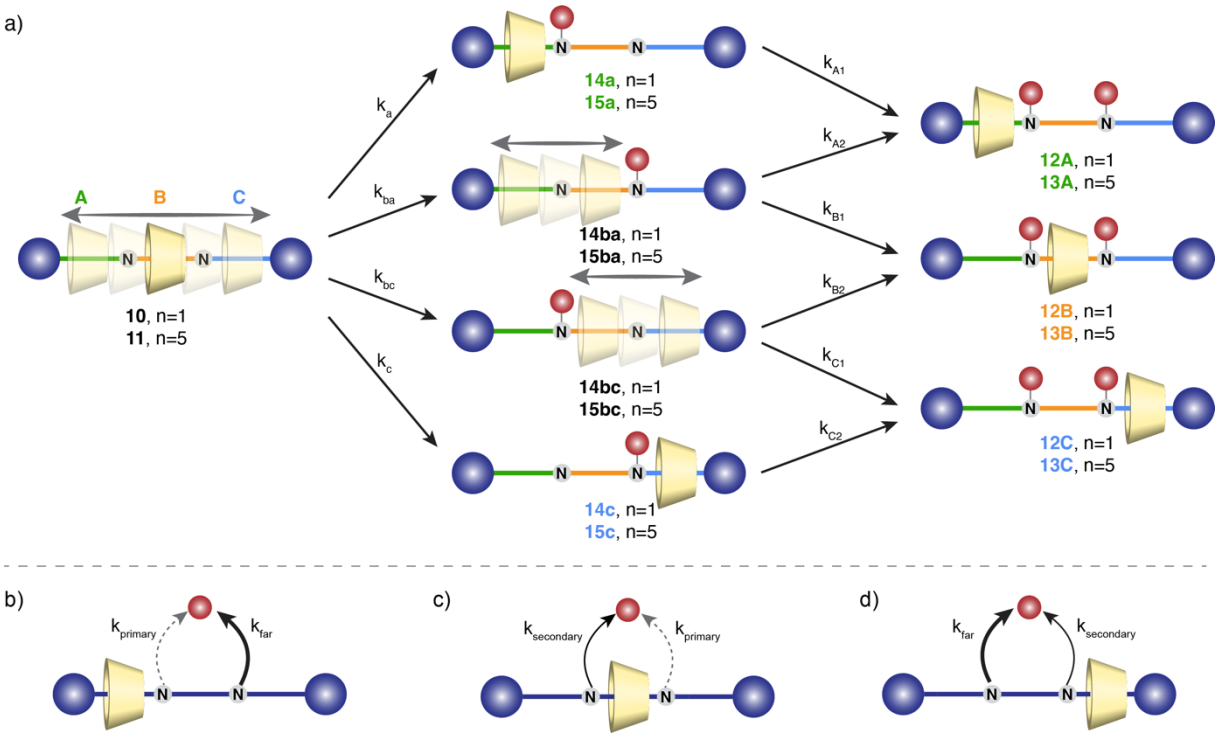

Scheme 6. a) Reaction pathway for the double Fmoc protection reaction. Proposed position b), d) and orientation c) kinetic biases controlling the information ratchet mechanism.

It has been shown, for both rotaxanes **10** and **11**, that the CD-occupancy of segment **C** is around 20%, regardless of the solvent. However, the Fmoc protection reaction produces a different distribution, which is dependent on the solvent, with an enrichment in the proportions of **12C** and **13C** formed. In the case of **11**, Fmoc protection was always slower when the small rim (as opposed to the large rim) of the CD faced the reacting nitrogen, resulting in the preferential formation of diastereoisomer **13C**. In the case of **10** the absence of isomer **12A** as a reaction product also clearly illustrated a kinetic reaction bias, resulting from the cone shape of the CD. The overall kinetics for the reaction of **10** are however complicated by the length of the lateral segments, which in turn influence the relative thermodynamic stabilities of the mechanoisomers, and reduce the preference for the formation of **12C** over **12B**. Nonetheless, these kinetic biases, brought out by the cone-shaped two-faced macrocycle employed as the movable entity in this system produce an information ratchet mechanism, wherein both the position and orientation of the CD influence the formation of kinetically favoured diastereoisomers.

Conclusion

In conclusion, we have developed a novel type of information ratchet, sensitive to two types of information, namely the position and orientation of the macrocycle threaded onto the molecular axle. The originality of this system comes from the intrinsic asymmetry of the cone-shaped chiral macrocycle, which presents two distinct faces towards a reactive site. The resulting kinetic biases, as assessed by analysis of product ratios, are clearly sensitive to both the position and orientation of the CD, as the

ratio of $k_{secondary}$ to $k_{primary}$ is dependent on its location on either segments **A**, **B** or **C** for both rotaxanes. Here, a double information input, induced by the asymmetric topography of macrocycle, has been achieved demonstrating the potential of asymmetric macrocycles to induce unidirectional motion. This new ratcheting mechanism may therefore be suited for application in a chemically fuelled unidirectional rotatory motor, similar to that previously disclosed by Leigh, but, thanks to the intrinsic chirality of the CD, with directionality information already embedded. An added advantage of the cone shape of CD's lies in the possibility of face-selective functionalisation. In particular, as envisioned by Leigh and Penocchio in an exploratory theoretical paper,[45] the addition of a catalyst either onto the small rim to accelerate deprotection, or onto the large rim to accelerate protection, should greatly improve the kinetic asymmetry and efficiency of the system. Such an endeavour is clearly now feasible, since the application of CDs in an in an information ratchet mechanism has been demonstrated and methods for their selective functionalization are well-known.[46,47] Moreover, the use of water-soluble CDs allows to consider operating this ratchet in aqueous media. This new information ratchet thus offers new possibilities for the design of molecular motors.

Author Contributions

EL, SC and LB performed the syntheses. EL, SC and CT recorded and analysed the NMR spectra. EL analysed the results and performed kinetic simulations. BH supervised SC and EL and contributed in the design and analysis of the results. MS and GV designed the study, supervised it and wrote the paper. All authors contributed to the writing of the paper.

Acknowledgements

The authors thank Cyclolab (Hungary) for generous supply of α-CD, Aurélie Bernard and Régina Maruchenko for efficient assistance in NMR, Agence Nationale de la Recherche (CycloMMotor ANR-22-CE07-0035) for financial support, and Prof. A. J. Fairbanks for proofreading the manuscript.

References

1. Balzani, V., Venturi, M., and Credi, A. (2008). Molecular Devices and Machines: Concepts and Perspectives for the Nanoworld (Wiley-VCH: Weinheim).
2. Erbas-Cakmak, S., Leigh, D.A., McTernan, C.T., and Nussbaumer, A.L. (2015). Artificial Molecular Machines. Chem. Rev. *115*, 10081-10206. 10.1021/acs.chemrev.5b00146.
3. Cheng, C., McGonigal, P.R., Schneebeli, S.T., Li, H., Vermeulen, N.A., Ke, C., and Stoddart, J.F. (2015). An artificial molecular pump. Nature Nanotech. *10*, 547-553. 10.1038/nnano.2015.96.
4. Amano, S., Fielden, S.D.P., and Leigh, D.A. (2021). A catalysis-driven artificial molecular pump. Nature *594*, 529-534. 10.1038/s41586-021-03575-3.
5. Ragazzon, G., Baroncini, M., Silvi, S., Venturi, M., and Credi, A. (2015). Light-powered autonomous and directional molecular motion of a dissipative self-assembling system. Nat Nano *10*, 70-75. 10.1038/nnano.2014.260.
6. Kottas, G.S., Clarke, L.I., Horinek, D., and Michl, J. (2005). Artificial Molecular Rotors. Chem. Rev. *105*,

1281-1376.

7. Jiménez, M.C., Dietrich-Buchecker, C., and Sauvage, J.-P. (2000). Towards Synthetic Molecular Muscles: Contraction and Stretching of a Linear Rotaxane Dimer. Angew. Chem. Int. Ed. *39*, 3284-3287. 10.1002/1521-3773(20000915)39:18<3284::AID-ANIE3284>3.0.CO;2-7.
8. von Delius, M., Geertsema, E.M., and Leigh, D.A. (2010). A synthetic small molecule that can walk down a track. Nat. Chem. *2*, 96-101. 10.1038/nchem.481.
9. Armaroli, N., Balzani, V., Collin, J.P., Gavina, P., Sauvage, J.P., and Ventura, B. (1999). Rotaxanes Incorporating Two Different Coordinating Units in Their Thread: Synthesis and Electrochemically and Photochemically Induced Molecular Motions. J. Am. Chem. Soc. *121*, 4397-4408.
10. Brouwer, A.M., Frochot, C., Gatti, F.G., Leigh, D.A., Mottier, L., Paolucci, F., Roffia, S., and Wurpel, G.W.H. (2001). Reversible translational motion in a hydrogen-bonded molecular shuttle. Science *291*, 2124-2128.
11. Browne, W.R., and Feringa, B.L. (2011). Molecular Switches (Wiley-VHC).
12. Kassem, S., van Leeuwen, T., Lubbe, A.S., Wilson, M.R., Feringa, B.L., and Leigh, D.A. (2017). Artificial molecular motors. Chem. Soc. Rev. *46*, 2592-2621. 10.1039/C7CS00245A.
13. Kelly, T.R., De Silva, H., and Silva, R.A. (1999). Unidirectional rotary motion in a molecular system. Nature *401*, 150-152.
14. Koumura, N., Zijistra, R.W.J., Van Delden, R.A., Harada, N., and Feringa, B.L. (1999). Light-driven monodirectional molecule rotor. Nature *401*, 152-155.
15. Leigh, D.A., Wong, J.K.Y., Dehez, F., and Zerbetto, F. (2003). Unidirectional rotation in a mechanically interlocked molecular rotor. Nature *424*, 174-179.
16. van Delden, R.A., ter Wiel, M.K.J., Pollard, M.M., Vicario, J., Koumura, N., and Feringa, B.L. (2005). Unidirectional molecular motor on a gold surface. Nature *437*, 1337-1340. 10.1038/nature04127.
17. Perera, U.G.E., Ample, F., Kersell, H., Zhang, Y., Vives, G., Echeverria, J., Grisolia, M., Rapenne, G., Joachim, C., and Hla, S.W. (2013). Controlled clockwise and anticlockwise rotational switching of amolecular motor. Nature Nanotech. *8*, 46-51. 10.1038/nnano.2012.218.
18. Erbas-Cakmak, S., Fielden Stephen, D.P., Karaca, U., Leigh David, A., McTernan Charlie, T., Tetlow Daniel, J., and Wilson Miriam, R. (2017). Rotary and linear molecular motors driven by pulses of a chemical fuel. Science *358*, 340-343. 10.1126/science.aao1377.
19. Chatterjee, M.N., Kay, E.R., and Leigh, D.A. (2006). Beyond Switches: Ratcheting a Particle Energetically Uphill with a Compartmentalized Molecular Machine. J. Am. Chem. Soc. *128*, 4058-4073. 10.1021/ja057664z.
20. Wilson, M.R., Solà, J., Carlone, A., Goldup, S.M., Lebrasseur, N., and Leigh, D.A. (2016). An autonomous chemically fuelled small-molecule motor. Nature *534*, 235. 10.1038/nature18013.
21. Serreli, V., Lee, C.-F., Kay, E.R., and Leigh, D.A. (2007). A molecular information ratchet. Nature *445*, 523-527. 10.1038/nature05452.
22. Astumian, R.D., and Derényi, I. (1998). Fluctuation driven transport and models of molecular motors and pumps. Eur. Biophys. J. *27*, 474-489. 10.1007/s002490050158.
23. Astumian, R.D. (2019). Kinetic asymmetry allows macromolecular catalysts to drive an information ratchet. Nat. Commun. *10*, 3837. 10.1038/s41467-019-11402-7.
24. Lau, B., Kedem, O., Schwabacher, J., Kwasnieski, D., and Weiss, E.A. (2017). An introduction to ratchets in chemistry and biology. Materials Horizons *4*, 310-318. 10.1039/C7MH00062F.
25. Alvarez-Pérez, M., Goldup, S.M., Leigh, D.A., and Slawin, A.M.Z. (2008). A Chemically-Driven Molecular Information Ratchet. J. Am. Chem. Soc. *130*, 1836-1838. 10.1021/ja7102394.
26. Carlone, A., Goldup, S.M., Lebrasseur, N., Leigh, D.A., and Wilson, A. (2012). A Three-Compartment

Chemically-Driven Molecular Information Ratchet. J. Am. Chem. Soc. *134*, 8321-8323. 10.1021/ja302711z.

27. Borsley, S., Leigh, D.A., and Roberts, B.M.W. (2021). A Doubly Kinetically-Gated Information Ratchet Autonomously Driven by Carbodiimide Hydration. J. Am. Chem. Soc. *143*, 4414-4420. 10.1021/jacs.1c01172.
28. Cui, J.-S., Ba, Q.-K., Ke, H., Valkonen, A., Rissanen, K., and Jiang, W. (2018). Directional Shuttling of a Stimuli-Responsive Cone-Like Macrocycle on a Single-State Symmetric Dumbbell Axle. Angew. Chem. Int. Ed. *57*, 7809-7814. 10.1002/anie.201803349.
29. Stanier, C.A., Alderman, S.J., Claridge, T.D.W., and Anderson, H.L. (2002). Unidirectional Photoinduced Shuttling in a Rotaxane with a Symmetric Stilbene Dumbbell. Angew. Chem. Int. Ed. *41*, 1769-1772. 10.1002/1521-3773(20020517)41:10<1769::AID-ANIE1769>3.0.CO;2-N.
30. Wenz, G., Han, B.-H., and Müller, A. (2006). Cyclodextrin Rotaxanes and Polyrotaxanes. Chem. Rev. *106*, 782-817. 10.1021/cr970027+.
31. Hashidzume, A., Yamaguchi, H., and Harada, A. (2019). Cyclodextrin-Based Rotaxanes: from Rotaxanes to Polyrotaxanes and Further to Functional Materials. Eur. J. Org. Chem. *2019*, 3344-3357. 10.1002/ejoc.201900090.
32. Cherraben, S., Scelle, J., Hasenknopf, B., Vives, G., and Sollogoub, M. (2021). Precise Rate Control of Pseudorotaxane Dethreading by pH-Responsive Selectively Functionalized Cyclodextrins. Org. Lett. *23*, 7938-7942. 10.1021/acs.orglett.1c02940.
33. Fredy, J.W., Scelle, J., Guenet, A., Morel, E., Adam de Beaumais, S., Ménand, M., Marvaud, V., Bonnet, C.S., Tóth, E., Sollogoub, M., et al. (2014). Cyclodextrin Polyrotaxanes as a Highly Modular Platform for the Development of Imaging Agents. Chem. Eur. J. *20*, 10915-10920. 10.1002/chem.201403635.
34. Fredy, J.W., Scelle, J., Ramniceanu, G., Doan, B.-T., Bonnet, C.S., Tóth, É., Ménand, M., Sollogoub, M., Vives, G., and Hasenknopf, B. (2017). Mechanostereoselective One-Pot Synthesis of Functionalized Head-to-Head Cyclodextrin [3]Rotaxanes and Their Application as Magnetic Resonance Imaging Contrast Agents. Org. Lett. *19*, 1136-1139. 10.1021/acs.orglett.7b00153.
35. Hashidzume, A., Kuse, A., Oshikiri, T., Adachi, S., Okumura, M., Yamaguchi, H., and Harada, A. (2018). Toward a translational molecular ratchet: face-selective translation coincident with deuteration in a pseudo-rotaxane. Sci. Rep. *8*, 8950. 10.1038/s41598-018-27226-2.
36. Akae, Y., Koyama, Y., Sogawa, H., Hayashi, Y., Kawauchi, S., Kuwata, S., and Takata, T. (2016). Structural Analysis and Inclusion Mechanism of Native and Permethylated α-Cyclodextrin-Based Rotaxanes Containing Alkylene Axles. Chem. Eur. J. *22*, 5335-5341. 10.1002/chem.201504882.
37. Armspach, D., Ashton, P.R., Moore, C.P., Spencer, N., Stoddart, J.F., Wear, T.J., and Williams, D.J. (1993). The Self-Assembly of Catenated Cyclodextrins. Angew. Chem. Int. Ed. *32*, 854-858. 10.1002/anie.199308541.
38. King, J.F., Rathore, R., Lam, J.Y.L., Guo, Z.R., and Klassen, D.F. (1992). pH optimization of nucleophilic reactions in water. J. Am. Chem. Soc. *114*, 3028-3033. 10.1021/ja00034a040.
39. Jamieson, E.M.G., Modicom, F., and Goldup, S.M. (2018). Chirality in rotaxanes and catenanes. Chem. Soc. Rev. *47*, 5266-5311. 10.1039/C8CS00097B.
40. Kawaguchi, Y., and Harada, A. (2000). A Cyclodextrin-Based Molecular Shuttle Containing Energetically Favored and Disfavored Portions in Its Dumbbell Component. Org. Lett. *2*, 1353-1356. 10.1021/ol0055667.
41. Carella, A., Jaud, J., Rapenne, G., and Launay, J.-P. (2003). Technomimetic molecules: synthesis of ruthenium(ii) 1,2,3,4,5-penta(p-bromophenyl)cyclopentadienyl hydrotris(indazolyl)borate, an

organometallic molecular turnstile. Chem. Commun., 2434-2435. 10.1039/B307577J.

42. Seeman, J.I. (1983). Effect of conformational change on reactivity in organic chemistry. Evaluations, applications, and extensions of Curtin-Hammett Winstein-Holness kinetics. Chem. Rev. *83*, 83-134. 10.1021/cr00054a001.
43. Seeman, J.I. (1986). The Curtin-Hammett principle and the Winstein-Holness equation: new definition and recent extensions to classical concepts. J. Chem. Educ. *63*, 42. 10.1021/ed063p42.
44. Amano, S., Esposito, M., Kreidt, E., Leigh, D.A., Penocchio, E., and Roberts, B.M.W. (2022). Using Catalysis to Drive Chemistry Away from Equilibrium: Relating Kinetic Asymmetry, Power Strokes, and the Curtin–Hammett Principle in Brownian Ratchets. J. Am. Chem. Soc. *144*, 20153-20164. 10.1021/jacs.2c08723.
45. Amano, S., Esposito, M., Kreidt, E., Leigh, D.A., Penocchio, E., and Roberts, B.M.W. (2022). Insights from an information thermodynamics analysis of a synthetic molecular motor. Nat. Chem. *14*, 530-537. 10.1038/s41557-022-00899-z.
46. Wang, B., Zaborova, E., Guieu, S., Petrillo, M., Guitet, M., Blériot, Y., Ménand, M., Zhang, Y., and Sollogoub, M. (2014). Site-selective hexa-hetero-functionalization of α-cyclodextrin an archetypical C6-symmetric concave cycle. Nat Commun *5*, 5354. 10.1038/ncomms6354.
47. Liu, J., Wang, B., Przybylski, C., Bistri-Aslanoff, O., Ménand, M., Zhang, Y., and Sollogoub, M. (2021). Programmed Synthesis of Hepta-Differentiated β-Cyclodextrin: 1 out of 117655 Arrangements. Angew. Chem. Int. Ed. *60*, 12090-12096. 10.1002/anie.202102182.